Article

Cell Reports

Critical Roles of the Histone Methyltransferase MLL4/KMT2D in Murine Hepatic Steatosis Directed by ABL1 and PPARγ2

Graphical Abstract

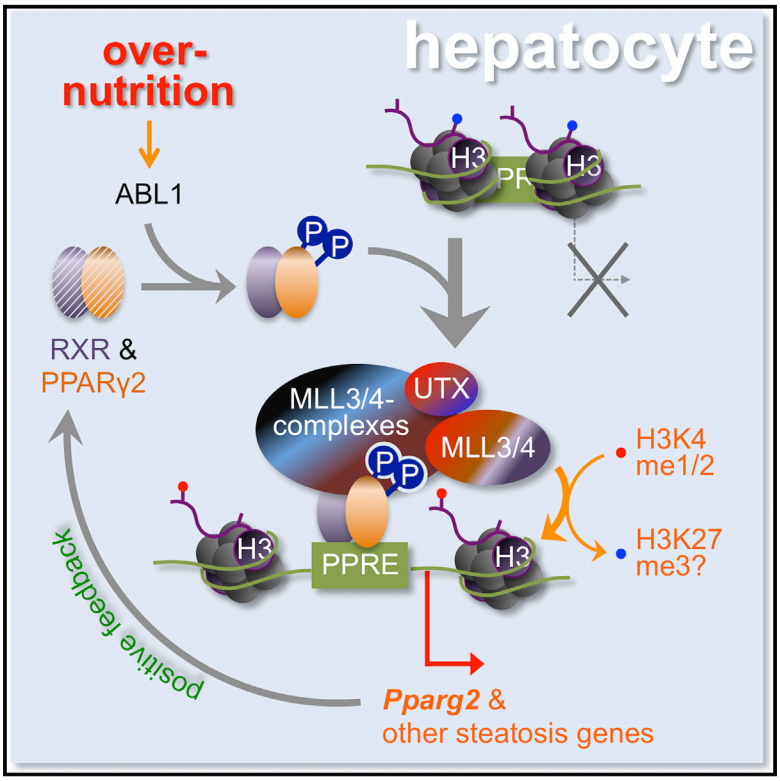

Authors

Dae-Hwan Kim, Janghyun Kim, Ji-Sun Kwon, ..., Soo-Kyung Lee, Seunghee Lee, Jae W. Lee

Correspondence

leeseung@snu.ac.kr (S.L.), leejae@ohsu.edu (J.W.L.)

In Brief

Kim et al. find that overnutrition-activated ABL1 kinase facilitates the association of the histone H3 lysine 4 methyltransferase MLL4 and PPARγ2, resulting in induction of the steatosis target genes of PPARγ2. They further show that imatinib, an ABL1 inhibitor, can dramatically improve the fatty liver condition of obese mouse models.

Highlights

- MLL4 is a critical epigenetic mediator of overnutrition-induced murine steatosis
- ABL1 kinase tethers MLL4 to PPARγ2, transactivating its steatotic target genes
- MLL4 also induces PPARγ2 because *Pparg2* itself is a target of the ABL1-PPARγ2-MLL4 axis
- ABL1 inhibition greatly improves the fatty liver condition of obese mouse models

Accession Numbers

GSE83940

Kim et al., 2016, Cell Reports *17*, 1671–1682
November 1, 2016
http://dx.doi.org/10.1016/j.celrep.2016.10.023

Cell Reports
Article

Critical Roles of the Histone Methyltransferase MLL4/KMT2D in Murine Hepatic Steatosis Directed by ABL1 and PPARγ2

Dae-Hwan Kim,[1] Janghyun Kim,[1] Ji-Sun Kwon,[1] Jaspreet Sandhu,[4] Peter Tontonoz,[4] Soo-Kyung Lee,[1,2] Seunghee Lee,[3,*] and Jae W. Lee[1,5,*]

[1]Neuroscience Section, Papé Family Pediatric Research Institute, Department of Pediatrics
[2]Vollum Institute
Oregon Health and Science University, Portland, OR 97239, USA
[3]College of Pharmacy and Research Institute of Pharmaceutical Sciences, Seoul National University, 08826 Seoul, Korea
[4]Department of Pathology and Laboratory Medicine, Howard Hughes Medical Institute, University of California, Los Angeles, Los Angeles, CA 90095, USA
[5]Lead Contact
*Correspondence: leeseung@snu.ac.kr (S.L.), leejae@ohsu.edu (J.W.L.)
http://dx.doi.org/10.1016/j.celrep.2016.10.023

SUMMARY

The pathophysiologic continuum of non-alcoholic fatty liver disease begins with steatosis. Despite recent advances in our understanding of the gene regulatory program directing steatosis, how it is orchestrated at the chromatin level is unclear. PPARγ2 is a hepatic steatotic transcription factor induced by overnutrition. Here, we report that the histone H3 lysine 4 methyltransferase MLL4/KMT2D directs overnutrition-induced murine steatosis via its coactivator function for PPARγ2. We demonstrate that overnutrition facilitates the recruitment of MLL4 to steatotic target genes of PPARγ2 and their transactivation via H3 lysine 4 methylation because PPARγ2 phosphorylated by overnutrition-activated ABL1 kinase shows enhanced interaction with MLL4. We further show that *Pparg2* (encoding PPARγ2) is also a hepatic target gene of ABL1-PPARγ2-MLL4. Consistently, inhibition of ABL1 improves the fatty liver condition of mice with overnutrition by suppressing the pro-steatotic action of MLL4. Our results uncover a murine hepatic steatosis regulatory axis consisting of ABL1-PPARγ2-MLL4, which may serve as a target of anti-steatosis drug development.

INTRODUCTION

Non-alcoholic fatty liver disease (NAFLD) shows a spectrum of liver pathology that resembles alcohol-induced fatty liver damage (Hardy et al., 2016). Because of its strong association with the widespread metabolic syndrome, NAFLD is also becoming epidemic and the leading cause of chronic liver disease in developed countries. Furthermore, a subset of individuals with NAFLD develop non-alcoholic steatohepatitis (NASH), and some of these NASH patients eventually develop cirrhosis and/or liver cancer (Hardy et al., 2016). In line with the notion that NAFLD is a major health risk, numerous studies have been performed to obtain a better understanding of the epidemiology, etiology, pathophysiology, and therapeutic intervention of the disease. In particular, triglyceride (TG) is an ester of three free fatty acids (FFAs) bound to glycerol, and the pathophysiologic continuum of NAFLD begins with accumulation of TGs within hepatocytes (i.e., hepatic steatosis). Despite great advances in our understanding of the gene regulatory program directing hepatic steatosis (Hardy et al., 2016), it is poorly understood how this program is orchestrated epigenetically.

We previously purified the two founding members of a family of the six mammalian SET1-like complexes (Lee et al., 2009) containing either the histone H3 lysine 4 methyltransferase (H3K4MT) mixed-lineage leukemia 3 (MLL3/KMT2C) or its closest paralog, MLL4/KMT2D (Goo et al., 2003; Lee et al., 2006). Each mammalian SET1-like complex contains one of the six H3K4MTs, SET1A/B and MLL1-4, complex-specific subunits, and a common subcomplex consisting of Rbbp5, Ash2l, Wdr5, and Dpy30, which facilitates the H3K4MT activity of SET1A/B/MLL1-4 (Lee et al., 2009). The MLL3/4 complexes were subsequently identified to also contain the histone H3 lysine 27 (H3K27) demethylase UTX (Agger et al., 2007; Hong et al., 2007; Lan et al., 2007; Lee et al., 2007; Smith et al., 2008). Their unique subunits, such as ASC-2/NCOA6 and PTIP, have been shown to serve as adaptors that recruit the non-DNA-binding epigenetic transcriptional coactivators MLL3/4 and UTX to enhancers of their target genes by directly interacting with specific transcription factors bound to those enhancers (Lee et al., 2009). In particular, ASC-2, using its two LXXLL motifs that recognize the activated conformation of nuclear receptors (NRs), has been suggested to tether MLL3/4/UTX to their target enhancers occupied by several NRs (Choi et al., 2005; Kim et al., 2003, 2009a, 2009b, 2015; Lee et al., 2006, 2008a, 2008b; Surapureddi et al., 2008),

triggering their target genes to form open chromatin for transactivation. Although UTX removes the repressive chromatin mark histone H3 lysine 27-trimethylation (H3K27me3) (Agger et al., 2007; Hong et al., 2007; Lan et al., 2007; Lee et al., 2007; Smith et al., 2008), MLL3/4 have been suggested to function through directing the mono- and di-methylation of H3K4 residues (histone H3 lysine 4-monomethylation/histone H3 lysine 4-dimethylation [H3K4me1/2]) of their target enhancers (Ang et al., 2016; Guo et al., 2013; Hu et al., 2013; Lee et al., 2013). Interestingly, epigenetic regulation of diverse metabolic processes has been defined as one of the key physiological functions of MLL3/4 complexes (Kim et al., 2003, 2009a, 2009b; Lee et al., 2008a, 2008b; Surapureddi et al., 2008). However, the exact identity of their target genes/enhancers responsible for each of these metabolic processes as well as the transcription factors that recruit MLL3/4 complexes to those genes remain to be further defined.

The NR, peroxisome proliferator activated receptor γ (PPARγ), is a master adipogenic transcription factor (Medina-Gomez et al., 2007; Vidal-Puig et al., 1996). The expression of PPARγ2, a more adipogenic isoform of PPARγ, is normally restricted to white and brown adipose tissue but ectopically induced in liver and skeletal muscle in response to overnutrition or genetic obesity (Medina-Gomez et al., 2007; Tontonoz et al., 1994; Vidal-Puig et al., 1996). Consistent with the notion that overnutrition causes endoplasmic reticulum (ER) stress (Hummasti and Hotamisligil, 2010), which results from a disequilibrium between the folding capacity of the ER and the amount of proteins to be folded, ER stress is observed in the lipid excess livers of *ob*/*ob* and high-fat diet (HFD)-fed mice (Ozcan et al., 2004). ER stress is also known to activate ABL1 kinase (Ito et al., 2001; Pattacini et al., 2004; Qi and Mochly-Rosen, 2008). Raising the interesting idea that ABL1 kinase is a key effector of fat storage in response to overnutrition, ABL1 kinase has recently been demonstrated to be a positive regulator of adipogenesis (Keshet et al., 2014). During adipogenesis, ABL1 binds to the PPARγ2 isoform-specific N-terminal region of PPARγ2 and phosphorylates two tyrosine residues in the AF1 domain of PPARγ2, which increases the protein stability of PPARγ2 as well as the binding affinity of PPARγ2 to its transcriptional coactivator, PPAR γ coactivator 1α (PGC1α), leading to an enhancement in PPARγ2 transactivation potential (Keshet et al., 2014).

In this report, using a combination of HFD-induced hepatic steatosis paradigm and unbiased genome-wide RNA sequencing (RNA-seq) analyses, we establish MLL4 as a critical regulator of overnutrition-induced hepatic steatosis. We also demonstrate that this function of MLL4 is mainly mediated by PPARγ2 because MLL4 preferentially binds to PPARγ2 over PPARγ1, likely via PPARγ2-specific phosphorylation by HFD-activated ABL1 kinase in the liver. We further show that imatinib, an ABL1 inhibitor, suppresses the pro-steatotic action of MLL4 and improves the fatty liver condition of *ob*/*ob* and HFD-fed mice. Overall, our results uncover a critical regulatory axis in overnutrition-directed hepatic steatosis and present this ABL1-PPARγ2-MLL3/4 axis as a potential target for anti-steatosis drug development.

RESULTS

Resistance of *Mll3/4* Mutant Mice to HFD-Induced Hepatic Steatosis

We have reported previously that homozygous mutant mice expressing a catalytically inactive deletion form of MLL3, named $Mll3^{\Delta/\Delta}$, are resistant to fatty liver formation induced by HFD (Lee et al., 2008a, 2008b). Because our previous studies indicated that MLL3 and MLL4 play similar roles in several metabolic processes (Kim et al., 2009a, 2015; Lee et al., 2008a, 2008b), we hypothesized that *Mll4* mutant mice may also show resistance to HFD-induced hepatic steatosis. Although our $Mll4^{-/-}$ mice displayed early embryonic lethality, $Mll4^{+/-}$ mice survived into adulthood (Kim et al., 2015). To test our hypothesis, we subjected $Mll4^{+/-}$ mice to 16 weeks of HFD feeding. Indeed, like $Mll3^{\Delta/\Delta}$ mice, $Mll4^{+/-}$ mice were resistant to HFD-induced hepatic steatosis (Figure 1A). Oil red O staining confirmed that $Mll4^{+/-}$ livers accumulated much less fat relative to wild-type (WT) littermate control livers after 16 weeks of HFD feeding (Figure 1B). These mouse genetic results suggest that MLL3 and MLL4 likely function similarly in directing fatty liver formation.

Critical Roles of MLL4 in HFD-Dependent Transcriptome Changes of the Mouse Liver

The dramatic difference between control and *Mll3/4* mutants in HFD-induced fatty liver formation (Figures 1A and 1B; Lee et al., 2008a, 2008b), together with the notion that MLL3/4 act as transcriptional coactivators, raises the interesting possibility that MLL3/4 may play critical roles in HFD-dependent transcriptome changes in the mouse liver. To test this idea, we performed RNA-seq using the livers of 8-week-old WT and $Mll4^{+/-}$ male mice fed either a normal chow diet (CD) or HFD for 8 weeks. These analyses identified 272 genes whose expression showed more than a 1.5-fold difference between CD- and HFD-fed WT livers (false discovery rate < 10%), consisting of 153 HFD-induced genes and 119 HFD-suppressed genes (Figure 1C). Among the 153 HFD-induced genes in WT livers, we identified 100 genes (~65%) whose expression was less efficiently upregulated by HFD in $Mll4^{+/-}$ livers (more than 1.5-fold change between $Mll4^{+/-}$ and WT under HFD conditions; false discovery rate < 10%; Figures 1C and 1D; Table S1). Among the 119 HFD-suppressed genes in WT livers, we identified 61 genes (~51%) whose expression was already downregulated in $Mll4^{+/-}$ livers under CD conditions (more than 1.5-fold change between $Mll4^{+/-}$ and WT; false discovery rate < 10%; Figures 1C and 1D; Table S2). These results demonstrate that the expression of a large portion of HFD-controlled genes (161 of 272 genes, ~60%) require MLL4, establishing a critical role for MLL4 in HFD-dependent transcriptome changes in the mouse liver.

Identification of Steatotic Genes as Major Targets of MLL3/4 in the Liver

Given the resistance of *Mll3/4* mutants to HFD-induced fatty liver formation, we hypothesized that the HFD-dependent transcriptome changes of the mouse liver directed by MLL4 (Figures 1C and 1D) likely involve hepatic steatotic genes. We

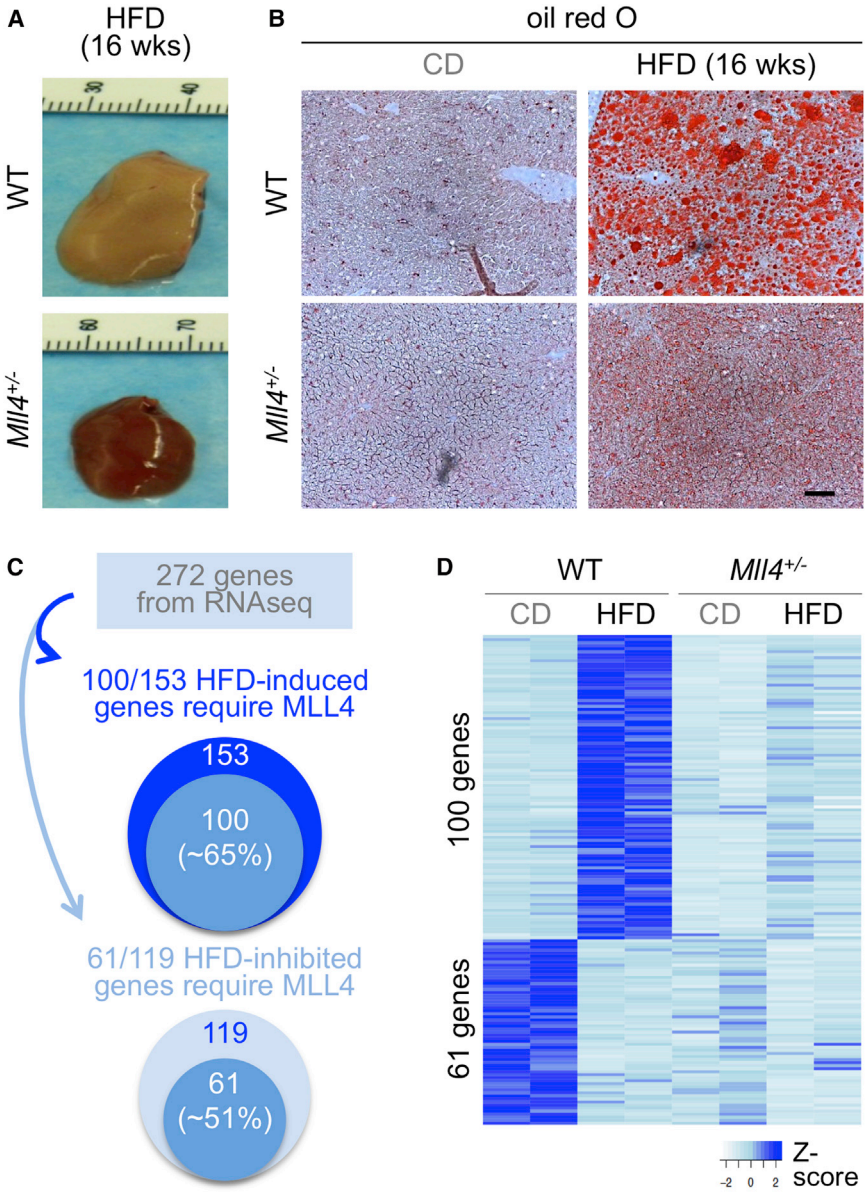

Figure 1. Resistance of *Mll4*$^{+/-}$ Mice to HFD-Induced Steatosis

(A) Gross morphology of livers from WT and *Mll4*$^{+/-}$ mice fed an HFD for 16 weeks.

(B) Oil red O staining to visualize lipids in the livers in (A). Scale bar, 100 μm.

(C) Schematic of the notion that a significant portion of HFD-regulated genes require MLL4 in their response to an HFD.

(D) Heatmap for genes that require MLL4 for their up- or downregulation by an HFD.

See also Tables S1 and S2.

recently determined the transcriptome changes in the livers of 5-month-old WT, *Mll3*$^{+/\Delta}$, *Mll4*$^{+/-}$, and *Mll3*$^{+/\Delta}$;*Mll4*$^{+/-}$ mice using RNA-seq, identifying genes that are either positively or negatively regulated by MLL3/4 in the liver (Kim et al., 2015). In support of our hypothesis, gene ontology (GO) analyses of the positively regulated target genes of MLL3/4 revealed the GO term "lipid synthesis" (Kim et al., 2015). Surprisingly, further analysis of the genes in this GO category disclosed that they belong to three specific input pathways for hepatic FFAs and TGs; i.e., FFA uptake, de novo fatty acid synthesis, and lipid droplet synthesis (Figure 2A). Moreover, an identical GO term (i.e., lipid synthesis) and a similar set of genes were also identified from further analysis of the 100 HFD-inducible genes that required MLL4 (Figure 2B; Figure S1A). Notably, the 161 HFD-induced/repressed genes produced only four prominent GO terms, and the GO term for lipid synthesis was statistically most significant (Figure S1A). Some of these RNA-seq results were independently validated (Figures S1B—S1D). Our results suggest that specific activation of the expression of genes involved in input pathways for hepatic FFAs and TGs is a major mechanism MLL3/4 employ to direct hepatic steatosis.

PPARγ as a Key Mediator of the Hepatic Steatotic Function of MLL4

Because the MLL3/4 complexes are transcriptional coactivators that recognize their target genes via DNA-bound transcription factors, we hypothesized that known and/or unknown steatotic transcription factors expressed in the liver recruit MLL3/4 complexes to their steatotic target genes. To test this idea, we first considered several well defined hepatic steatotic transcription factors, including ChREBP, SREBP1c, the liver X receptors (LXRs, consisting of LXRα and LXRβ), and PPARγ. Although the LXRs and PPARγ have been reported previously to associate with MLL3/4 complexes (Lee et al., 2008a, 2008b), we failed to detect any interaction of MLL3/4 complexes with ChREBP and SREBP1c (Figure S2A). Although the expression of many of our steatotic genes was not induced under the "high-fat and carbohydrate diet" condition (60% fat, 20% carbohydrate) as opposed to our HFD condition (42% fat, 0.2% cholesterol), it was drastically impaired in *Lxrα/β* double knockout livers (Figures S2B–S2D). These results prompt us to further investigate whether LXRs are involved with recruiting MLL3/4 complexes to their target steatotic genes under our HFD paradigm. However, several lines of evidence strongly suggested that PPARγ acts as a major transcription factor that recruits MLL3/4 complexes to many of their hepatic steatotic target genes. First, we examined the recently reported chromatin immunoprecipitation sequencing (ChIP-seq) peaks for MLL4 and PPARγ during adipogenesis (Lee

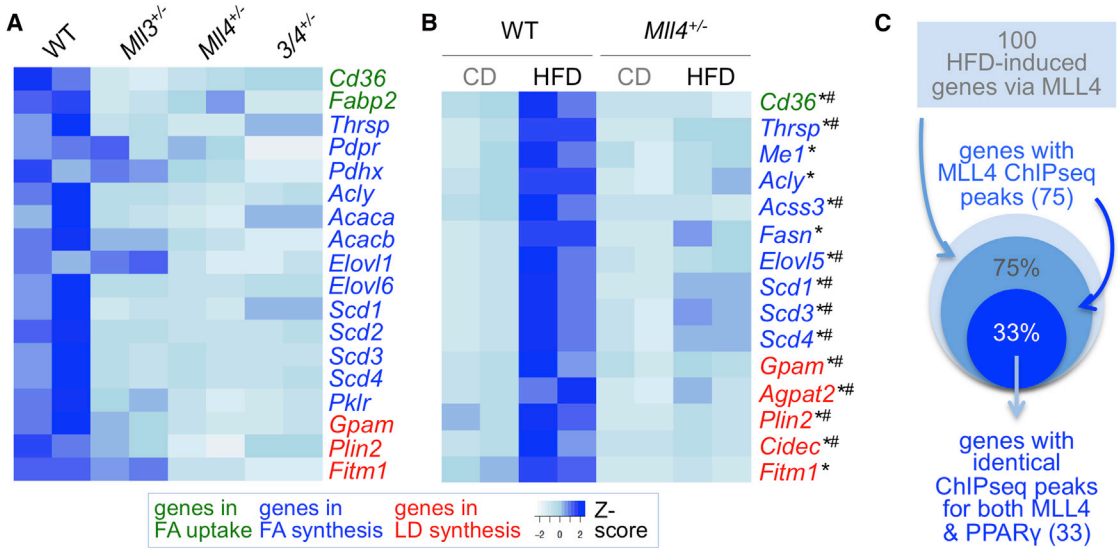

Figure 2. Steatotic Target Genes of MLL3/4

(A) Heatmap for clustering of steatotic target genes of MLL3/4 into three input pathways for fatty liver formation (Kim et al., 2015).

(B) Heatmap for clustering of HFD-induced steatotic target genes of MLL4 into three input pathways for fatty liver formation.

(C) Schematic of the notion that a significant portion of HFD-induced genes contain ChIP-seq peaks for both MLL4 and PPARγ.

See also Figures S1–S3.

et al., 2013) because genome-wide ChIP-seq studies for MLL4 and PPARγ in fatty livers have not yet been reported, and adipogenesis and hepatic steatosis share a similar gene regulatory program (Memon et al., 2000; Okumura, 2011). Strikingly, all of our 15 steatotic genes had ChIP-seq peaks for MLL4 (indicated by * in Figure 2B and Figure S3), and 11 of these genes (over 73%) showed identical ChIP-seq peaks for both MLL4 and PPARγ (indicated by # in Figure 2B and Figure S3). In addition, among our 100 high fat diet-induced genes, 75 genes (75%) displayed ChIP-seq peaks for MLL4, whereas 33 genes (33%) had identical ChIP-seq peaks for both MLL4 and PPARγ (Figure 2C; Table S1). Second, PPARγ has been reported to directly activate the expression of at least three of our identified steatotic genes: *Cd36* (Tontonoz et al., 1998), *Plin2* (Fan et al., 2009; Kang et al., 2015), and *Cidec* (Kim et al., 2008; Matsusue et al., 2008). Third, in the mouse liver carcinoma cell line Hepa1c1c7, which has been widely utilized as a surrogate cell line to study liver biology (Bernhard et al., 1973), the expression of three of our identified steatotic genes, *Scd1*, *Cd36*, and *Cidec*, was induced by the PPARγ ligand rosiglitazone, and these inductions were impaired by co-transfected small hairpin RNA (shRNA) construct against MLL4 (Figure 3A). Fourth, similar inductions were also observed with livers from WT mice when 30 mg/kg of rosiglitazone was given by daily intraperitoneal injection for 7 days, whereas these hepatic inductions were significantly dampened in *Mll4*$^{+/-}$ mice (Figure 3B).

Taken together, these results strongly suggest that PPARγ is a major transcription factor that recruits MLL3/4 complexes to a large fraction of the HFD-inducible target genes of MLL4 (Table S1), including those involved in promoting fatty liver formation (Figure 2B).

Transactivation of Steatotic Target Genes of the MLL4 Complex via PPARγ in the Liver

To investigate whether PPARγ is indeed responsible for recruiting MLL3/4 complexes to their steatotic target genes, we first focused on *Cd36* in Hepa1c1c7 cells. Among multiple regions of *Cd36* containing identical ChIP-seq peaks for both MLL4 and PPARγ as well as the PPAR response element (PPRE) during adipogenesis (Lee et al., 2013), we found that a region approximately 25 kb upstream of the transcription start site (indicated by a red arrow in Figure 3A and Figure S4) recruits both PPARγ and MLL4 in a PPARγ ligand (rosiglitazone)-enhanced manner in Hepa1c1c7 cells (Figure 4A), coincident with an increase in H3K4me1 levels (Figure 4B). Moreover, H3K4me1 levels were significantly dampened by shRNA against MLL4 (Figure 4B), demonstrating that decoration of this *Cd36*-PPRE region by H3K4me1 is carried out by MLL4. In addition, occupancy of the same region of *Cd36* by MLL4 was significantly enhanced by 8 weeks of HFD feeding in WT livers (Figure 4C). The HFD-enhanced recruitment of MLL4 to the *Cd36*-PPRE region was coincident with an increase in H3K4me1 levels, whereas this increase was significantly abolished in *Mll4*$^{+/-}$ livers (Figure 4D). Further, recruitment of MLL4 to the *Cd36*-PPRE region was significantly induced in the livers of WT mice when 30 mg/kg of rosiglitazone was given by daily intraperitoneal injection for 7 days (Figure 4E). Similar results were also obtained for PPREs in two additional steatotic target genes of MLL3/4 complexes, *Scd1* and *Cidec* (Figures 4F and 4G; Figures S3H, S3L, and S4). For these experiments, we used a homemade rabbit antibody against MLL4 whose specificity toward MLL4 was validated by immunoblotting, immunoprecipitation, and immunostaining of liver tissues (Figures S2A, S5A, and S5B).

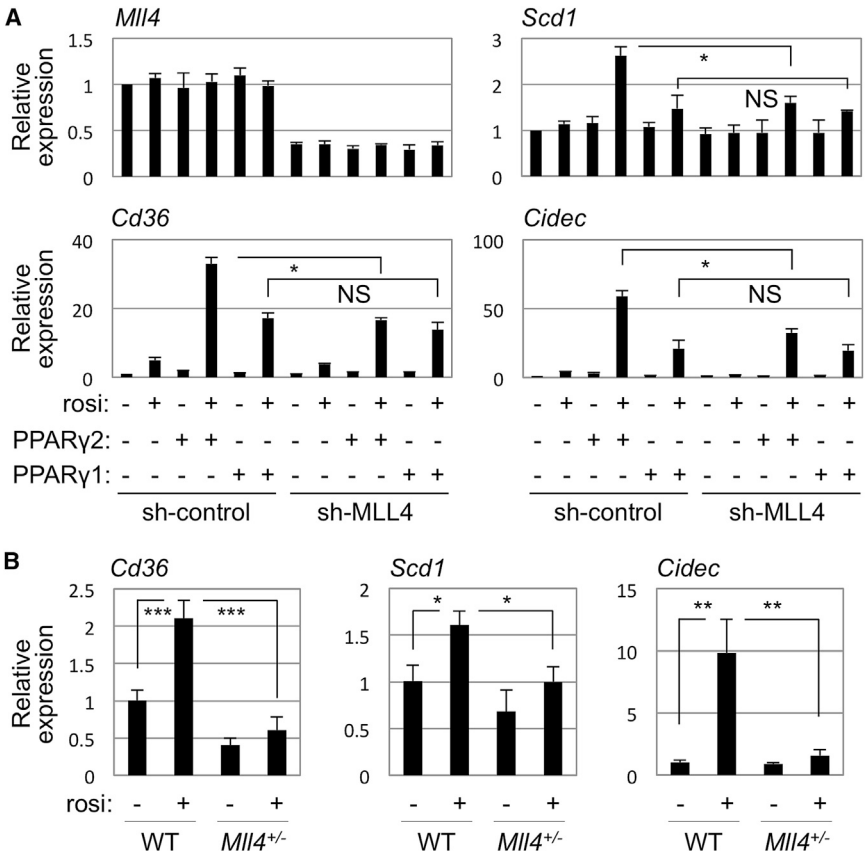

Figure 3. Critical Roles of MLL4 in the Hepatic Expression of Steatotic Genes

(A) In Hepa1c1c7 hepatocarcinoma cells, rosiglitazone, a PPARγ ligand, enhances the expression of three steatotic target genes of MLL4 (*Cd36*, *Scd1*, and *Cidec*) directed by both PPARγ1 and PPARγ2. Knockdown of MLL4 levels using sh-MLL4 impairs the induction of these genes by PPARγ2 but not by PPARγ1. Knockdown of MLL4 was also examined as shown.

(B) Intraperitoneal injection of rosiglitazone results in induction of the expression of *Cd36*, *Scd1*, and *Cidec* in WT mice but not in *Mll4*$^{+/-}$ mice (n = 4 for each data point).

All errors are SD.

Taken together, these results suggest that PPARγ plays critical roles in recruiting MLL3/4 complexes to their hepatic steatotic target genes and that MLL3/4, in turn, direct H3K4me1 decoration of their target enhancer regions.

Pparg2 as a Hepatosteatotic Target Gene of the MLL4 Complex

Because PPARγ2 (Figure 5A) is a nutritionally regulated isoform of PPARγ (Medina-Gomez et al., 2007; Vidal-Puig et al., 1996), and the MLL4 complex was found to play critical roles in HFD-dependent transcriptome changes in the mouse liver (Figure 1C), we hypothesized that the expression of PPARγ2 is either directly or indirectly regulated by the MLL4 complex. In support of this idea, the expression of PPARγ2, but not PPARγ1, was induced by HFD in WT livers but much less robustly in *Mll4*$^{+/-}$ livers (Figure 5B). Interestingly, two prominent overlapping ChIP-seq peaks for both PPARγ and MLL4 were found around the PPARγ2 promoter region (Figure 5C, peaks A and B). Each peak contains a highly conserved PPRE around its summit region (Figure S4), raising the interesting possibility that PPARγ may autoregulate transactivation of the PPARγ2 promoter by employing the MLL4 complex as a coactivator. Consistent with this idea, HFD feeding triggered MLL4 recruitment to both peaks (Figure 5D). The HFD-dependent recruitment of MLL4 to *Pparg*-PPRE-A concurred with its H3K4me1 decoration in WT livers, whereas HFD feeding failed to robustly induce H3K4me1 decoration in this region in *Mll4*$^{+/-}$ livers (Figure 5E). In addition, the expression of PPARγ2 (but not PPARγ1) was readily induced in WT livers when 30 mg/kg of rosiglitazone was given by daily intraperitoneal injection for 7 days (Figure 5F), which was coincidental with recruitment of MLL4 to *Pparg*-PPRE-A (Figure 5G).

These results, together with our findings that PPARγ2 is an abundant isoform under HFD conditions (Figure 5B) and that MLL4 is required for transactivation by PPARγ2 but not PPARγ1 (Figure 3A), suggest that, in response to lipid excess, PPARγ2 (rather than PPARγ1) regulates the expression of PPARγ2 by recruiting MLL4 to the *Pparg2* promoter region, identifying *Pparg2* as a steatotic target gene of the MLL4 complex in the liver.

ABL1 Kinase Enhances the Ability of PPARγ2 to Interact with MLL4 in Hepa1c1c7 Cells

Given the central roles of PPARγ2 in adipogenesis and HFD-induced fatty liver formation, we further hypothesized that the MLL4 complex may selectively interact with PPARγ2 and act as a PPARγ2-selective coactivator. In support of this idea, rosiglitazone-dependent transactivation of the expression of *Scd1*, *Cd36*, and *Cidec* by PPARγ2 in Hepa1c1c7 cells was impaired by sh-MLL4, whereas their transactivation by PPARγ1 was not affected by sh-MLL4 (Figure 3A). To further test our hypothesis, we transfected Hepa1c1c7 cells with FLAG epitope-tagged PPARγ2 and PPARγ1, followed by immunoprecipitation with either control immunoglobulin G (IgG) or anti-MLL4 antibody. Interestingly, we found that association of PPARγ1/2 and MLL4 requires rosiglitazone that and MLL4 co-immunopurified PPARγ2 more robustly than PPARγ1 (27% of input versus 5% of input; Figure 6A). Moreover, in Hepa1c1c7 cells, although MLL4-PPARγ2 interactions were only slightly increased in the presence of BCR-ABL fusion protein, a constitutively active form of ABL1 (24% of input versus 32% of input; Figure 6B), they were dampened by imatinib, an inhibitor of ABL1 kinase, in both the absence and presence of BCR-ABL (24% of input to 12% of input without BCR-ABL and 32% of input to 9% of input with BCR-ABL; Figure 6B). These results suggest that

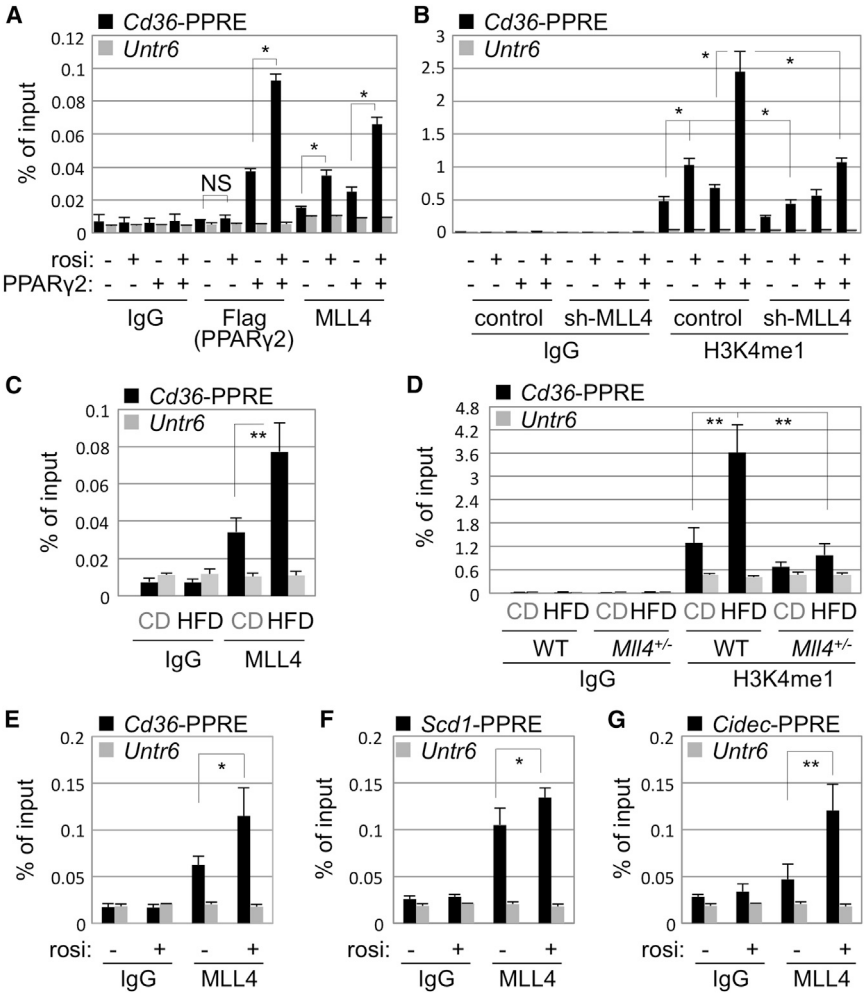

Figure 4. Critical Roles of PPARγ in Activation of the Steatotic Target Genes of MLL4

(A) ChIP for rosiglitazone-enhanced recruitment of PPARγ2 and MLL4 to *Cd36*-PPRE in Hepa1c1c7 cells transfected with FLAG-tagged PPARγ2.

(B) ChIP for rosiglitazone/PPARγ2-enhanced H3K4me1 levels in *Cd36*-PPRE in Hepa1c1c7 cells transfected with scrambled control shRNA or sh-MLL4.

(C) ChIP for HFD-enhanced recruitment of MLL4 to *Cd36*-PPRE in WT livers (n = 4 for each data point).

(D) ChIP for HFD-enhanced H3K4me1 levels in *Cd36*-PPRE in WT livers but not in *Mll4*$^{+/-}$ livers (n = 4 for each data point).

(E–G) ChIP for rosiglitazone-enhanced recruitment of MLL4 to *Cd36*-PPRE (E), Scd1-PPRE (F), and *Cidec*-PPRE (G) in WT livers (n = 4 for each data point).

The genomic region *Untr6* was used as a negative control throughout all ChIP experiments performed. All errors are SD. See also Figure S4.

PPARγ2-MLL4 interactions may be enhanced by ABL1-dependent phosphorylation of PPARγ2, as described recently for another coactivator of PPARγ2, PGC1α (Keshet et al., 2014). Consistent with this idea, relative to WT PPARγ2, MLL4 interacted slightly more efficiently with a mutant form of PPARγ2 in which the two tyrosine phosphorylation sites by ABL1 were replaced by phosphorylation mimicking glutamic acid (20% of input to 28% of input; Figure 6C). In contrast, MLL4 interacted less efficiently with a PPARγ2 mutant in which the two tyrosine phosphorylation sites were replaced by non-phosphorylatable phenylalanine (20% of input to 9% of input; Figure 6C). These results strongly suggest that ABL1-dependent phosphorylation of PPARγ2 enhances the association of PPARγ2 with the MLL4 complex in Hepa1c1c7 liver carcinoma cells.

HFD Enhances the Transactivation Potential of PPARγ2-MLL4 in the Liver via ABL1

During adipogenesis, ABL1 kinase has been reported to enhance both the protein stability of PPARγ2 and the ability of PPARγ2 to interact with its coactivator PGC1α (Keshet et al., 2014). To further test whether ABL1 similarly enhances the transactivation potential of PPARγ2-MLL4 in the liver, we first monitored whether HFD feeding results in activation of ABL1 in mouse livers. Interestingly, in WT livers, the levels of ABL1 itself and PPARγ2 were increased with HFD feeding, whereas the levels of the α-actin loading control did not change (Figure 6D). To test whether the increase in PPARγ2 levels is due to an increase in ABL1 levels, we performed daily intraperitoneal injection of 50 mg/kg of the ABL1 inhibitor imatinib into HFD-fed mice for 5 consecutive days (Figure 6D) or *ob/ob* mice for 4 consecutive days (Figure 6E). Under both conditions, we observed a significant decrease in both ABL1 and PPARγ2 levels, whereas the levels of α-actin and/or Rbbp5, a common subunit of Set1-like complexes, did not change significantly (Figures 6D and 6E). Given the positive correlation between ABL1 and PPARγ2 levels (Figures 6D and 6E), we speculate that HFD-induced ABL1 in WT livers (Figure 6D) or ABL1 in *ob/ob* livers (Figure 6E) is likely an activated form. However, an activated form of ABL1 (ABL1, phosphorylated at tyrosine 245 or 412, which is readily detected with BCR-ABL) was very difficult to detect in the liver. We reasoned that, relative to BCR-ABL, a constitutively activated form of ABL, phosphorylation levels of endogenous ABL1 at tyrosine 245 or 412 may be much lower or dynamically regulated in the liver.

To determine whether ABL1 also enhances the association of PPARγ2 with the MLL4 complex, we performed co-immunoprecipitation experiments between PPARγ2 and MLL4 complex-specific subunits such as ASC-2 and PTIP using the above *ob/ob* livers treated with vehicle alone or imatinib. However, these experiments were not conclusive because of technical difficulty. However, we found that imatinib decreases the association of PPARγ2 and Rbbp5 (8% of input to 1% of input, arrowheads in Figure 6F), under a condition for comparable

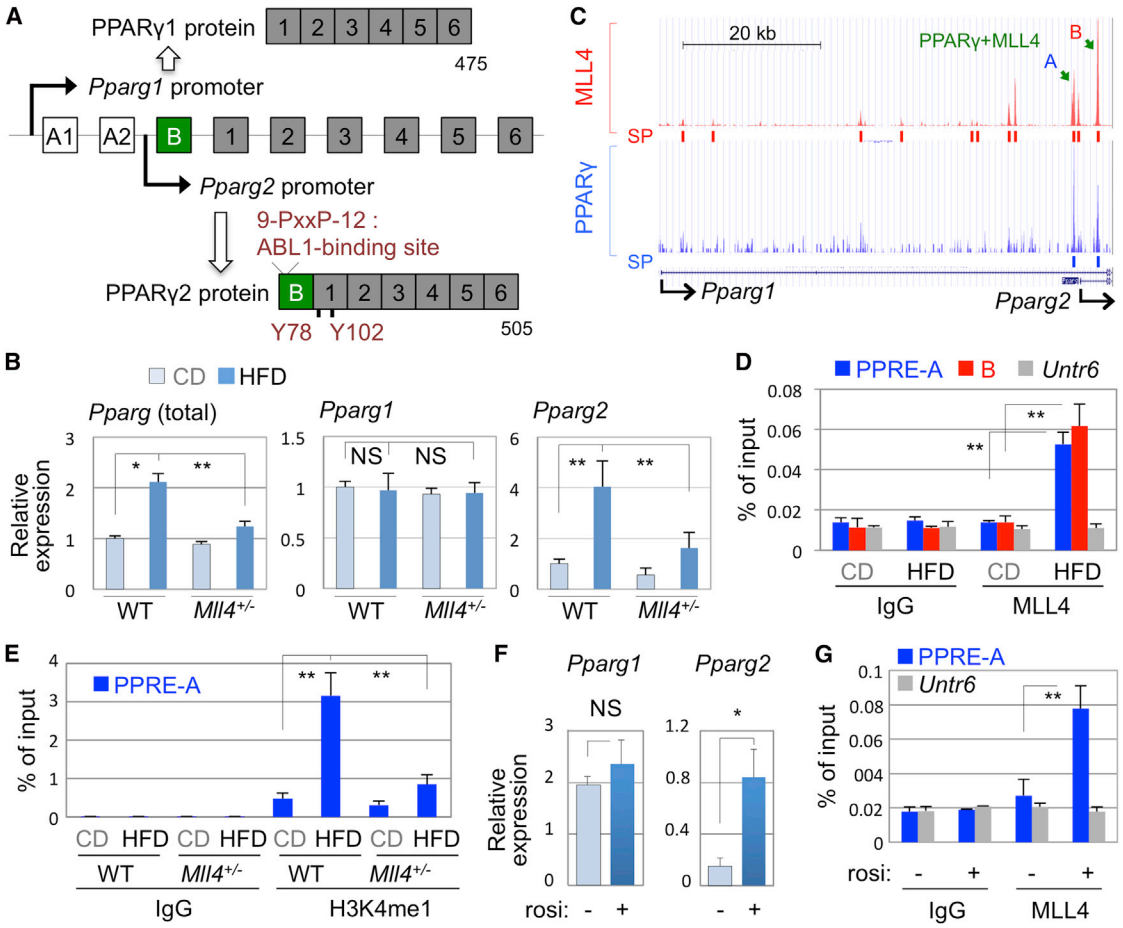

Figure 5. *Pparg2* as a Hepatic Steatotic Target Gene of PPARγ2-MLL4

(A) Schematic of PPARγ1 and PPARγ2 proteins and their genes as well as the known ABL1 kinase-binding site (PXXP) and two tyrosine residues phosphorylated by ABL1.

(B) qRT-PCR assessment of the expression levels of PPARγ1 and PPARγ2 in the WT liver under normal CD and HFD feeding conditions using primers specific to each isoform and primers that detect both isoforms (n = 4 for each data point).

(C) Schematic of ChIP peaks for MLL4 and PPARγ in the *Pparg* locus. Two MLL4 peaks overlapping with PPARγ peaks at identical regions are highlighted as A and B peaks.

(D) ChIP for HFD-enhanced recruitment of MLL4 to *Pparg*-PPRE-A and *Pparg*-PPRE-B in WT livers (n = 4).

(E) ChIP for HFD-enhanced H3K4me1 levels in *Pparg*-PPRE-A in WT livers, which is almost abolished in *Mll4*$^{+/-}$ livers (n = 4 for each data point).

(F) The expression levels of PPARγ1 and PPARγ2 in WT livers injected with vehicle or rosiglitazone (n = 4 for each data point).

(G) ChIP for rosiglitazone-enhanced recruitment of MLL4 to *Pparg*-PPRE-A in WT livers (n = 4 for each data point). The genomic region *Untr6* was used as a negative control.

Errors are SD in (B) and (D)—(G).

immunoprecipitation efficiency of PPARγ2 (48% of input versus 43% of input, arrows in Figure 6F). These results strongly suggest that ABL1 kinase is likely needed for the association of PPARγ2 with the MLL4 complex in lipid excess *ob/ob* livers.

Although it remains to be determined how imatinib leads to a decrease in ABL1 levels, our results raise the interesting possibility that HFD feeding activates ABL1 kinase in the liver and enhances the transactivation potential of PPARγ2-MLL4, likely via phosphorylation of PPARγ2, which may contribute to both stabilization of PPARγ2 and its enhanced association with the MLL4 complex, similar to the findings observed during adipogenesis (Keshet et al., 2014). Given that *Pparg2* itself is a target gene of PPARγ2-MLL4 (Figure 5), it is also possible that the imatinib-directed decrease in PPARγ2 levels (Figures 6D and 6E) may result only from suppression of the transactivation potential of PPARγ2-MLL4 because of loss of the interactions between PPARγ2 and the MLL4 complex and not from affecting the protein stability of PPARγ2.

Imatinib Improves the Fatty Liver Condition of *ob/ob* and HFD-Fed Mice at Least in Part by Antagonizing Recruitment of MLL4 to PPREs in Steatotic Target Genes of MLL4

Based on the potentially critical roles of ABL1 kinase for transactivation potential of PPARγ2-MLL4 (Figure 6), we hypothesized that imatinib will be a powerful inhibitor of the steatotic action

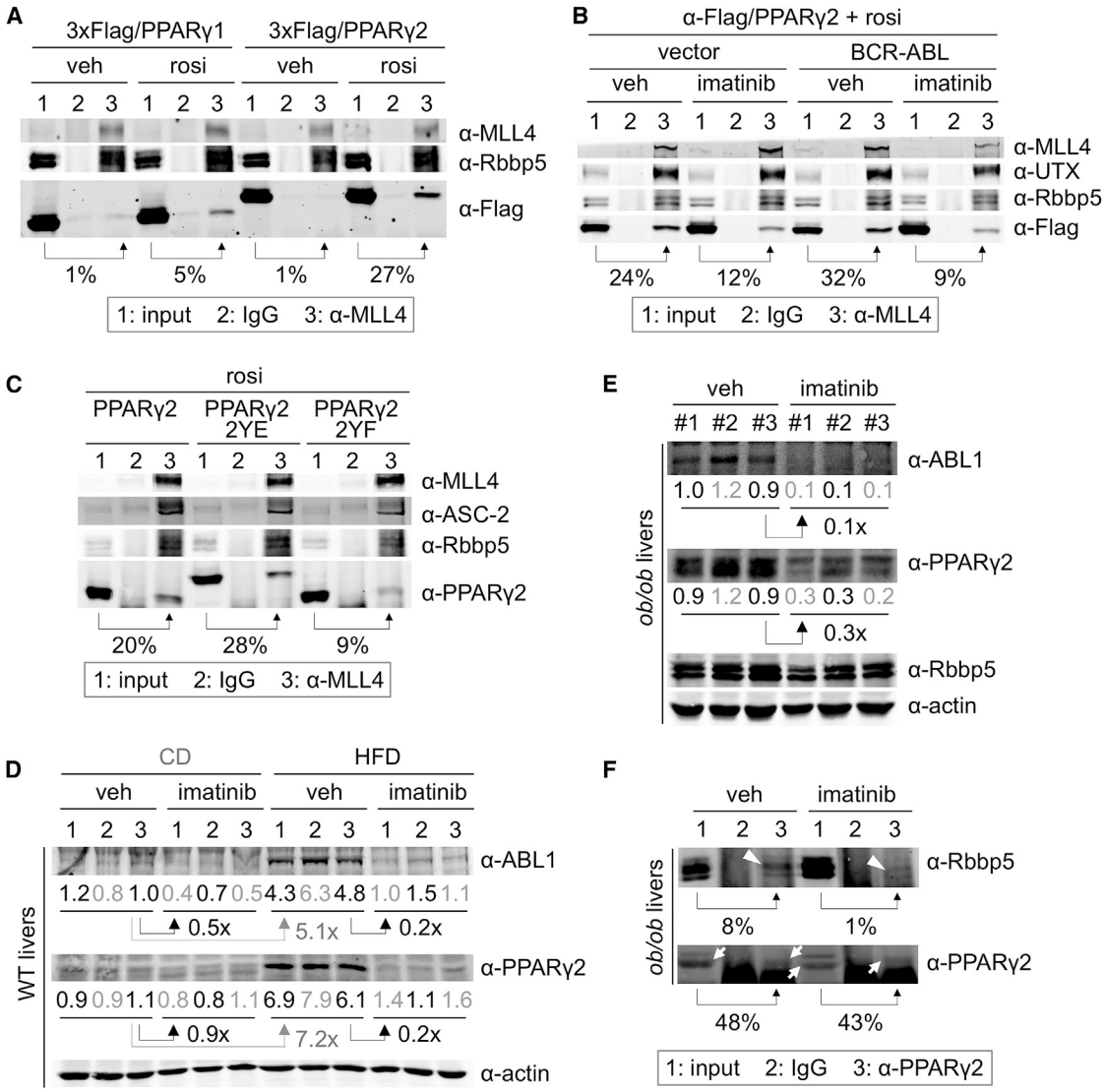

Figure 6. Roles of ABL1 Kinase in PPARγ2 Levels and Association of PPARγ2 and the MLL4 Complex

(A) In Hepa1c1c7 cells transfected with FLAG-tagged PPARγ1 and PPARγ2, MLL4 shows rosiglitazone-dependent interactions with both PPARγ1 and PPARγ2, but the interactions with PPARγ2 are much stronger than those with PPARγ1.

(B) In Hepa1c1c7 cells transfected with FLAG-tagged PPARγ2, coexpression of BCR-ABL slightly enhances the interaction between MLL4 and PPARγ2, whereas imatinib blunts these interactions both in the absence and presence of BCR-ABL.

(C) In Hepa1c1c7 cells, MLL4 showed interactions with FLAG-tagged WT PPARγ2, which became slightly stronger with PPARγ2-2YE but blunted with PPARγ2-2YF.

(D) Livers from WT mice fed either CD or HFD for 8 weeks and then subjected to daily injection of vehicle alone or imatinib for 5 consecutive days were immunoblotted with antibodies against ABL1, PPARγ2, and α-actin. The band intensity of ABL1 and PPARγ2 was quantified in comparison with that of α-actin using ImageJ.

(E) Livers from *ob/ob* mice injected with vehicle alone or imatinib for 4 consecutive days were immunoblotted with antibodies against ABL1, PPARγ2, Rbbp5, and α-actin. The band intensity of ABL1 and PPARγ2 was quantified in comparison with that of α-actin using ImageJ.

(F) Liver lysates from *ob/ob* mice injected with vehicle alone or imatinib for 4 consecutive days were immunoprecipitated with anti-PPARγ2 antibody, followed by immunoblotting with anti-Rbbp5 and anti-PPARγ2 antibodies. Arrowheads, Rbbp5; arrows, PPARγ2. The band intensity of Rbbp5 and PPARγ2 was quantified using ImageJ.

of PPARγ2-MLL4 in the liver. In support of this idea, recruitment of MLL4 to *Pparg*-PPRE-A as well as *Cd36*-PPRE, *Cidec*-PPRE, and *Scd1*-PPRE in *ob/ob* livers was significantly dampened by daily intraperitoneal injection of 50 mg/kg of an ABL1 inhibitor, imatinib, for 4 consecutive days (Figure 7A; Figure S5C). In addition, the expression of *Scd1* and *Pparg2*, two steatotic target genes of PPARγ2-MLL4, in *ob/ob* livers was strikingly decreased with 4 days of imatinib treatment (Figure 7B). The expression of other steatotic target genes of PPARγ2-MLL4, such as *Cd36*, *Cidec*, and *Plin2*, also showed a tendency to decrease, whereas

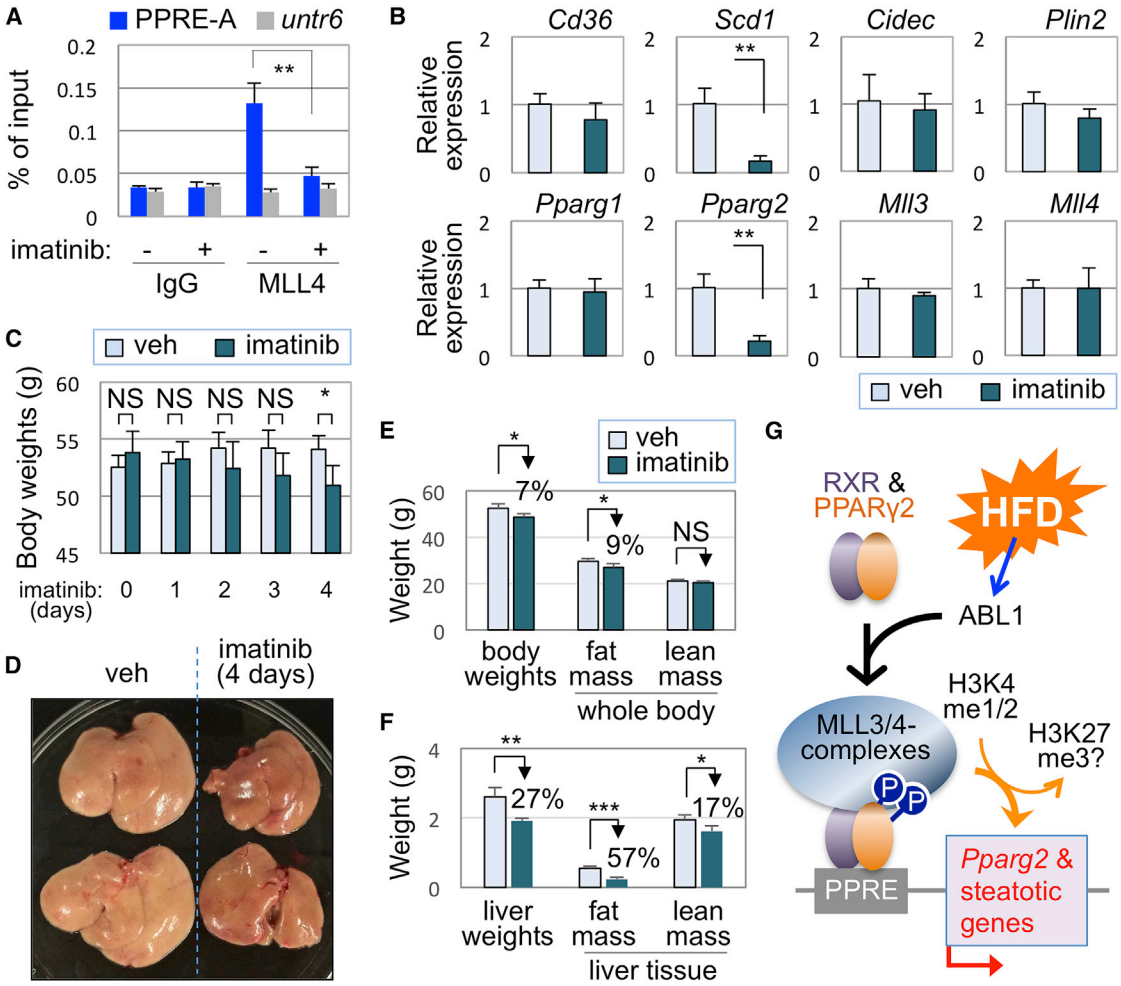

Figure 7. Improvement of the Fatty Liver Condition of *ob/ob* Mice by Imatinib

(A) ChIP experiments with *ob/ob* mice injected with vehicle alone or imatinib reveal that association of MLL4 with *Pparg*-PPRE-A in *ob/ob* livers is abolished by imatinib. ChIP experiments against the genomic region *untr6* were done as a negative control.

(B) Expression of the steatotic target genes of PPARγ2-MLL4 in *ob/ob* livers injected with either vehicle alone or imatinib for 4 consecutive days (n = 4 for each treatment).

(C) Body weights were measured for *ob/ob* mice injected once a day with vehicle alone or imatinib for 4 consecutive days.

(D) Gross morphology of livers of *ob/ob* mice after daily injection of vehicle alone or imatinib for 4 consecutive days.

(E) MRI measurement of whole-body fat mass and lean mass after daily injection of vehicle alone or imatinib for 4 consecutive days. Body weights were also measured.

(F) MRI measurement of liver fat mass and lean mass after daily injection of vehicle alone or imatinib for 4 consecutive days. Liver weights were also measured.

(G) Working model for roles of the ABL1-PPARγ2-MLL4 axis in HFD-induced steatosis. HFD activates ABL1 kinase activity, which, in turn, increases the protein levels of PPARγ2 and/or the interactions of PPARγ2 with the MLL4 complex, resulting in transactivation of steatotic target genes of the PPARγ2-MLL4 complex. This involves decoration of steatotic target genes of PPARγ2-MLL4 with H3K4me1/2 using the MLL4 subunit of the MLL4 complex, and it remains to be determined whether removal of H3K27me3 by UTX is also involved with this transactivation process.

Errors are SD in (A)–(C) (E), and (F). See also Figures S5–S7.

imatinib failed to affect the expression levels of MLL3, MLL4, and PPARγ1 (Figure 7B). In addition, when we performed daily injection of 50 mg/kg of imatinib into HFD-fed mice for 5 consecutive days, we observed a significant reduction in the expression of four of the five steatosis target genes of MLL3/4 we examined (Figure S6A).

Based on these results, we predicted that imatinib will improve the fatty liver condition of *ob/ob* and HFD-fed mice. In support of this idea, by day 4 of imatinib treatment, we observed that *ob/ob* mice showed a significant decrease in body weight (Figure 7C) as well as a significant improvement in liver color (i.e., more reddish/less fatty with imatinib; Figure 7D). Interestingly, although imatinib treatment reduced the total body weight by ~7%, it decreased the liver weight by ~27% (Figures 7E and 7F), suggesting that imatinib may affect the liver more selectively than other organs. In support of this idea, our MRI measurement of fat and lean mass revealed that imatinib treatment results in a 9% decrease in whole-body fat mass and that it reduces liver

fat mass by 57% (Figures 7E and 7F). Notably, the 9% reduction in whole-body fat mass in *ob*/*ob* mice is not visually evident (Figure S7), suggesting that imatinib-directed improvement in fatty liver is not due to lack of overall body fats. Similarly, by days 4 and 5 of imatinib treatment, HFD-fed mice showed a significant decrease in body weight (loss of ~7% and ~9% of body weight relative to vehicle-treated controls, respectively; Figure S6B). However, imatinib did not affect food intake (Figure S6C) but resulted in a dramatic change in liver color (i.e., more reddish/less fatty with imatinib; Figure S6D) as well as a significant decrease in liver weight (Figure S6E).

Taken together, our results suggest that ABL1 inhibition leads to a significant decrease in fat mass in the liver, likely through interfering with the hepatic steatotic regulatory axis consisting of ABL1-PPARγ2-MLL4, although it also results in a less prominent but still significant decrease in the whole-body fat mass, supporting a report implicating ABL1 in adipogenesis (Keshet et al., 2014). Our results also suggest that the hepatic ABL1-PPARγ2-MLL4 axis is perhaps a valuable drug development target for treating steatosis and NAFLD.

DISCUSSION

Overnutrition, such as an HFD or genetic obesity, triggers NAFLD, whose pathophysiologic continuum begins with steatosis (Hardy et al., 2016). Steatosis results from an imbalance between FFA/TG acquisition and removal. FFAs/TGs are acquired from the diet, de novo lipogenesis, and peripheral tissues, and dietary carbohydrates also activate de novo lipogenesis, whereas removal of FFAs/TGs involves mitochondrial β-oxidation, assembly of VLDL with apoB for secretion into the blood, and incorporation into phospholipids and other lipids (Hardy et al., 2016). In this report, using unbiased RNA-seq analyses, we made two remarkable discoveries. First, we found that the hepatic expression of approximately 60% of HFD-controlled genes requires MLL4 (Figure 1C), establishing MLL4 as a critical player in overnutrition-induced transcriptome changes in the mouse liver. Second, we found that MLL3/4 activate the expression of genes involved with three input pathways for hepatic FFAs/TGs (i.e., FFA uptake from the periphery, lipogenesis, and TG synthesis/storage) but not any of the output pathways (Figures 2A and 2B; Figure S1A), identifying MLL3/4 as major drivers of hepatic steatosis. Interestingly, it was recently suggested that MLL4 plays more dominant roles than MLL3 in adipogenesis and myogenesis (Lee et al., 2013). Furthermore, the potent resistance to HFD-induced hepatic steatosis associated with $Mll4^{+/-}$ and $Mll3^{\Delta/\Delta}$ mice was not observed in our $Mll3^{+/\Delta}$ mice (Lee et al., 2008a). Taken together, we believe that, although MLL3 and MLL4 play similar roles in overnutrition-induced hepatic steatosis, MLL4 is likely a dominant player in triggering hepatic steatosis.

The striking specificity of MLL3/4 toward three input pathways for hepatic FFAs/TGs likely reflects the ability of MLL3/4 complexes to physically recognize only a specific subset of transcription factors. In support of this idea, among multiple steatotic transcription factors, we discovered that the MLL4 complex interacts with PPARγ (Figure 6A). Our RNS-seq results indeed suggested that PPARγ plays critical roles in recruiting the MLL4 complex to many of the HFD-regulated target genes of MLL4, including genes involved with steatosis (Figures 2B and 2C; Tables S1 and S2). Interestingly, our results further revealed that PPARγ2 but not PPARγ1 likely recruits the MLL4 complex to its steatotic target genes during overnutrition-induced steatosis. First, PPARγ2 showed a 5.4-fold higher affinity than PPARγ1 in interactions with the MLL4 complex (Figure 6A). Second, MLL4 is required for transactivation of its steatotic target genes by PPARγ2 but not by PPARγ1 in the Hepa1c1c7 hepatocarcinoma cell line (Figure 3A). Third, the expression of PPARγ2 but not PPARγ1 is highly induced under our HFD condition, resulting in 4-fold higher levels of PPARγ2 than of PPARγ1 (Figure 5B). Coupled with the higher affinity of PPARγ2 toward the MLL4 complex, this can result in a 21.6-fold (5.4- × 4-fold) higher chance for PPARγ2 to associate with the MLL4 complex in comparison with PPARγ1. Fourth, ABL1 kinase is known to enhance the association of PPARγ2 with its coactivator PGC1α via phosphorylation of PPARγ2 during adipogenesis (Keshet et al., 2014), and, similarly, we found that imatinib, an ABL1 kinase inhibitor, decreases the association of PPARγ2 with MLL4 in Hepa1c1c7 cells (Figure 6B), suggesting that imatinib impinges on the interactions of PPARγ2 with the MLL4 complex. We believe that this involves blocking the phosphorylation of PPARγ2 by ABL1 kinase because PPARγ2-MLL4 associations were dampened by mutation of two tyrosine residues that are phosphorylated by ABL1 kinase to non-phosphorylatable phenylalanine (Figure 6C). Of note, transfection of identical amounts of our expression vectors for PPARγ1 and PPARγ2 into Hepa1c1c7 cells resulted in approximately 4- to 5-fold higher levels of PPARγ2 proteins in comparison with PPARγ1 protein levels. Combined with the similar affinity of WT PPARγ2 and activated PPARγ2-2YE mutant toward MLL4 (Figure 6C), these results raise the interesting possibility that ABL1 in Hepa1c1c7 cells may be a constitutively activated mutant form. Although the two phosphorylated tyrosine residues in PPARγ2 are expected to be either directly or indirectly involved in interacting with one or more subunits of MLL3/4 complexes, the identity of the PPARγ2-interacting subunits and the molecular nature of the interaction interface remain to be determined. Fifth, we found that HFD activates ABL1 kinase in the liver (Figure 6D), and intraperitoneal injection of imatinib into *ob*/*ob* mice or HFD-fed mice led to a dramatic reduction in PPARγ2 levels in their livers (Figures 6D and 6E). Moreover, imatinib drastically reduced recruitment of MLL4 to its steatotic target genes in *ob*/*ob* mice (Figure 7A; Figure S5C). These results strongly support crucial roles of PPARγ2 in recruiting the MLL4 complex to its steatotic target genes. Overall, our results identify an interesting regulatory axis in hepatic steatosis consisting of overnutrition-induced ABL1 kinase, PPARγ2-specific phosphorylation by ABL1 and the resulting increase in the protein stability of PPARγ2 and/or in the binding affinity of PPARγ2 toward MLL4 complex, and transactivation of steatotic target genes of the PPARγ2-MLL4 complex (Figure 7G).

Epigenetic regulation of steatosis has been poorly understood. Our identification of the ABL-PPARγ2-MLL4 axis begins to provide critical insights into this issue. Through this axis, overnutrition such as an HFD or genetic obesity results in steatosis by mobilizing the MLL4 complex to the hepatic steatotic target genes of PPARγ2-MLL4, which, in turn, facilitates their open

chromatin formation. In particular, we have shown that recruitment of the MLL4 complex leads to an increase in the open chromatin mark H3K4me1 (Figures 4B and 4D and 5E), and it remains to be determined in the future whether UTX in the MLL4 complex also plays important roles in hepatic steatosis via its ability to remove the repressive chromatin mark H3K27me3 (Figure 7G).

PPARγ2 is a nutrition-induced factor in both adipogenesis and hepatic steatosis. Although the molecular basis for this induction during adipogenesis has been relatively well characterized (Rosen, 2005), little is known about how the expression of PPARγ2 is induced in response to overnutrition in the liver. Our results suggest that *Pparg2* itself is a direct target gene of the ABL1-PPARγ2-MLL4 axis. First, the promoter region of *Pparg2* contains at least two common ChIP-seq peaks for both MLL4 and PPARγ (Figure 5C), which we found to recruit MLL4 in response to HFD feeding (Figure 5D), concomitant with an MLL4-dependent increase in H3K4me1 levels (Figure 5E). Rosiglitazone treatment also triggered recruitment of MLL4 to these peaks in the liver, confirming that they represent functional PPRE for PPARγ (Figure 5G). Second, in response to HFD, the expression of PPARγ2 but not PPARγ1 was induced in the liver (Figure 5B). Moreover, inhibition of ABL1 kinase activity in *ob/ob* or HFD-fed livers led to a striking reduction in PPARγ2 mRNA levels (Figure 7B; Figure S6A) with a concomitant decrease in MLL4 recruitment to the *Pparg2* promoter region (Figure 7A).

In summary, this study identifies a critical regulatory axis in overnutrition-directed steatosis, and we also present this ABL1-PPARγ2-MLL4 axis as a potential target for anti-steatosis drug development. In addition to ABL1 inhibitors, any small molecule that antagonizes the H3K4MT enzymatic activity of MLL4 may improve the fatty liver condition of NAFLD patients. However, other steatotic transcription factors may also play roles in recruiting MLL3/4 complexes to their steatotic target genes. In particular, MLL3/4 complexes may be involved with de novo lipogenesis directed by the LXRs in the liver (Figure S2B–S2D; Hong and Tontonoz, 2014). Future studies should be directed at testing this possibility as well as identifying additional steatotic transcription factors that mediate the hepatic steatotic function of MLL3/4 complexes. Finally, it should be noted that imatinib, although it was originally developed as a specific inhibitor of BCR-ABL, also inhibits other tyrosine kinase receptors (Buchdunger et al., 2002). These include platelet-derived growth factor (PDGF) receptor, which mediates the steatosis action of PDGF-C (Campbell et al., 2005). Therefore, it remains to be determined whether the powerful anti-steatotic action of imatinib described in this study also involves additional tyrosine kinase receptors.

EXPERIMENTAL PROCEDURES

Animals

All mouse work was performed under an approved protocol by the Institutional Animal Care and Use Committee of the Oregon Health and Science University. Additional information regarding animals and other experiments is provided in the Supplemental Experimental Procedures.

Statistical Analysis

Statistical differences were determined by Student's t test. Statistical significance is displayed as follows: *$p < 0.05$, **$p < 0.01$, and ***$p < 0.001$.

ACCESSION NUMBERS

The accession number for the RNA-seq results reported in this paper is GEO: GSE83940.

SUPPLEMENTAL INFORMATION

Supplemental Information includes Supplemental Experimental Procedures, seven figures, and two tables and can be found with this article online at http://dx.doi.org/10.1016/j.celrep.2016.10.023.

AUTHOR CONTRIBUTIONS

D.H.K., J.K., J.S.K., and J.S. conducted the experiments. P.T., S.K.L, S.L., and J.W.L. designed the experiments. D.H.K., S.L., and J.W.L. wrote the paper.

ACKNOWLEDGMENTS

We thank Dr. Yosef Shaul for mutant PPARγ2 plasmids and Dr. So Yun Park for isolating total RNA from the livers of mice fed chow or a high-fat diet. This research was supported by grants from NIH/NINDS (R01 NS054941 to S.K.L.) and NIH/NIDDK (R01 DK064678 to J.W.L. and R01 DK103664 to S.K.L. and J.W.L.), Basic Science Research Program (NRF-2015R1A2A1A15055611), Bio and Medical Technology Development Program (NRF-2012M3A9C6050508), and the Global Core Research Center funded by the Korean government (MSIP) (2011-0030001) through the National Research Foundation of Korea funded by the Ministry of Science, ICT, and Future Planning.

Received: April 18, 2016
Revised: September 12, 2016
Accepted: October 7, 2016
Published: November 1, 2016

REFERENCES

Agger, K., Cloos, P.A., Christensen, J., Pasini, D., Rose, S., Rappsilber, J., Issaeva, I., Canaani, E., Salcini, A.E., and Helin, K. (2007). UTX and JMJD3 are histone H3K27 demethylases involved in HOX gene regulation and development. Nature *449*, 731–734.

Ang, S.Y., Uebersohn, A., Spencer, C.I., Huang, Y., Lee, J.E., Ge, K., and Bruneau, B.G. (2016). KMT2D regulates specific programs in heart development via histone H3 lysine 4 di-methylation. Development *143*, 810–821.

Bernhard, H.P., Darlington, G.J., and Ruddle, F.H. (1973). Expression of liver phenotypes in cultured mouse hepatoma cells: synthesis and secretion of serum albumin. Dev. Biol. *35*, 83–96.

Buchdunger, E., O'Reilly, T., and Wood, J. (2002). Pharmacology of imatinib (STI571). Eur. J. Cancer *38*, S28–S36.

Campbell, J.S., Hughes, S.D., Gilbertson, D.G., Palmer, T.E., Holdren, M.S., Haran, A.C., Odell, M.M., Bauer, R.L., Ren, H.P., Haugen, H.S., et al. (2005). Platelet-derived growth factor C induces liver fibrosis, steatosis, and hepatocellular carcinoma. Proc. Natl. Acad. Sci. USA *102*, 3389–3394.

Choi, E., Lee, S., Yeom, S.Y., Kim, G.H., Lee, J.W., and Kim, S.W. (2005). Characterization of activating signal cointegrator-2 as a novel transcriptional coactivator of the xenobiotic nuclear receptor constitutive androstane receptor. Mol. Endocrinol. *19*, 1711–1719.

Fan, B., Ikuyama, S., Gu, J.Q., Wei, P., Oyama, J., Inoguchi, T., and Nishimura, J. (2009). Oleic acid-induced ADRP expression requires both AP-1 and PPAR response elements, and is reduced by Pycnogenol through mRNA degradation in NMuLi liver cells. Am. J. Physiol. Endocrinol. Metab. *297*, E112–E123.

Goo, Y.H., Sohn, Y.C., Kim, D.H., Kim, S.W., Kang, M.J., Jung, D.J., Kwak, E., Barlev, N.A., Berger, S.L., Chow, V.T., et al. (2003). Activating signal cointegrator 2 belongs to a novel steady-state complex that contains a subset of trithorax group proteins. Mol. Cell. Biol. *23*, 140–149.

Guo, C., Chen, L.H., Huang, Y., Chang, C.C., Wang, P., Pirozzi, C.J., Qin, X., Bao, X., Greer, P.K., McLendon, R.E., et al. (2013). KMT2D maintains neoplastic cell proliferation and global histone H3 lysine 4 monomethylation. Oncotarget *4*, 2144–2153.

Hardy, T., Oakley, F., Anstee, Q.M., and Day, C.P. (2016). Nonalcoholic Fatty Liver Disease: Pathogenesis and Disease Spectrum. Annu. Rev. Pathol. *11*, 451–496.

Hong, C., and Tontonoz, P. (2014). Liver X receptors in lipid metabolism: opportunities for drug discovery. Nat. Rev. Drug Discov. *13*, 433–444.

Hong, S., Cho, Y.W., Yu, L.R., Yu, H., Veenstra, T.D., and Ge, K. (2007). Identification of JmjC domain-containing UTX and JMJD3 as histone H3 lysine 27 demethylases. Proc. Natl. Acad. Sci. USA *104*, 18439–18444.

Hu, D., Gao, X., Morgan, M.A., Herz, H.M., Smith, E.R., and Shilatifard, A. (2013). The MLL3/MLL4 branches of the COMPASS family function as major histone H3K4 monomethylases at enhancers. Mol. Cell. Biol. *33*, 4745–4754.

Hummasti, S., and Hotamisligil, G.S. (2010). Endoplasmic reticulum stress and inflammation in obesity and diabetes. Circ. Res. *107*, 579–591.

Ito, Y., Pandey, P., Mishra, N., Kumar, S., Narula, N., Kharbanda, S., Saxena, S., and Kufe, D. (2001). Targeting of the c-Abl tyrosine kinase to mitochondria in endoplasmic reticulum stress-induced apoptosis. Mol. Cell. Biol. *21*, 6233–6242.

Kang, Y., Hengbo, S., Jun, L., Jun, L., Wangsheng, Z., Huibin, T., and Huaiping, S. (2015). PPARG modulated lipid accumulation in dairy GMEC via regulation of ADRP gene. J. Cell. Biochem. *116*, 192–201.

Keshet, R., Bryansker Kraitshtein, Z., Shanzer, M., Adler, J., Reuven, N., and Shaul, Y. (2014). c-Abl tyrosine kinase promotes adipocyte differentiation by targeting PPAR-gamma 2. Proc. Natl. Acad. Sci. USA *111*, 16365–16370.

Kim, S.W., Park, K., Kwak, E., Choi, E., Lee, S., Ham, J., Kang, H., Kim, J.M., Hwang, S.Y., Kong, Y.Y., et al. (2003). Activating signal cointegrator 2 required for liver lipid metabolism mediated by liver X receptors in mice. Mol. Cell. Biol. *23*, 3583–3592.

Kim, Y.J., Cho, S.Y., Yun, C.H., Moon, Y.S., Lee, T.R., and Kim, S.H. (2008). Transcriptional activation of Cidec by PPARgamma2 in adipocyte. Biochem. Biophys. Res. Commun. *377*, 297–302.

Kim, D.H., Lee, J., Lee, B., and Lee, J.W. (2009a). ASCOM controls farnesoid X receptor transactivation through its associated histone H3 lysine 4 methyltransferase activity. Mol. Endocrinol. *23*, 1556–1562.

Kim, G.H., Park, K., Yeom, S.Y., Lee, K.J., Kim, G., Ko, J., Rhee, D.K., Kim, Y.H., Lee, H.K., Kim, H.W., et al. (2009b). Characterization of ASC-2 as an antiatherogenic transcriptional coactivator of liver X receptors in macrophages. Mol. Endocrinol. *23*, 966–974.

Kim, D.H., Rhee, J.C., Yeo, S., Shen, R., Lee, S.K., Lee, J.W., and Lee, S. (2015). Crucial roles of mixed-lineage leukemia 3 and 4 as epigenetic switches of the hepatic circadian clock controlling bile acid homeostasis in mice. Hepatology *61*, 1012–1023.

Lan, F., Bayliss, P.E., Rinn, J.L., Whetstine, J.R., Wang, J.K., Chen, S., Iwase, S., Alpatov, R., Issaeva, I., Canaani, E., et al. (2007). A histone H3 lysine 27 demethylase regulates animal posterior development. Nature *449*, 689–694.

Lee, S., Lee, D.K., Dou, Y., Lee, J., Lee, B., Kwak, E., Kong, Y.Y., Lee, S.K., Roeder, R.G., and Lee, J.W. (2006). Coactivator as a target gene specificity determinant for histone H3 lysine 4 methyltransferases. Proc. Natl. Acad. Sci. USA *103*, 15392–15397.

Lee, M.G., Villa, R., Trojer, P., Norman, J., Yan, K.P., Reinberg, D., Di Croce, L., and Shiekhattar, R. (2007). Demethylation of H3K27 regulates polycomb recruitment and H2A ubiquitination. Science *318*, 447–450.

Lee, J., Saha, P.K., Yang, Q.H., Lee, S., Park, J.Y., Suh, Y., Lee, S.K., Chan, L., Roeder, R.G., and Lee, J.W. (2008a). Targeted inactivation of MLL3 histone H3-Lys-4 methyltransferase activity in the mouse reveals vital roles for MLL3 in adipogenesis. Proc. Natl. Acad. Sci. USA *105*, 19229–19234.

Lee, S., Lee, J., Lee, S.K., and Lee, J.W. (2008b). Activating signal cointegrator-2 is an essential adaptor to recruit histone H3 lysine 4 methyltransferases MLL3 and MLL4 to the liver X receptors. Mol. Endocrinol. *22*, 1312–1319.

Lee, S., Roeder, R.G., and Lee, J.W. (2009). Roles of histone H3-lysine 4 methyltransferase complexes in NR-mediated gene transcription. Prog. Mol. Biol. Transl. Sci. *87*, 343–382.

Lee, J.E., Wang, C., Xu, S., Cho, Y.W., Wang, L., Feng, X., Baldridge, A., Sartorelli, V., Zhuang, L., Peng, W., and Ge, K. (2013). H3K4 mono- and di-methyltransferase MLL4 is required for enhancer activation during cell differentiation. eLife *2*, e01503.

Matsusue, K., Kusakabe, T., Noguchi, T., Takiguchi, S., Suzuki, T., Yamano, S., and Gonzalez, F.J. (2008). Hepatic steatosis in leptin-deficient mice is promoted by the PPARgamma target gene Fsp27. Cell Metab. *7*, 302–311.

Medina-Gomez, G., Gray, S.L., Yetukuri, L., Shimomura, K., Virtue, S., Campbell, M., Curtis, R.K., Jimenez-Linan, M., Blount, M., Yeo, G.S., et al. (2007). PPAR gamma 2 prevents lipotoxicity by controlling adipose tissue expandability and peripheral lipid metabolism. PLoS Genet. *3*, e64.

Memon, R.A., Tecott, L.H., Nonogaki, K., Beigneux, A., Moser, A.H., Grunfeld, C., and Feingold, K.R. (2000). Up-regulation of peroxisome proliferator-activated receptors (PPAR-alpha) and PPAR-gamma messenger ribonucleic acid expression in the liver in murine obesity: troglitazone induces expression of PPAR-gamma-responsive adipose tissue-specific genes in the liver of obese diabetic mice. Endocrinology *141*, 4021–4031.

Okumura, T. (2011). Role of lipid droplet proteins in liver steatosis. J. Physiol. Biochem. *67*, 629–636.

Ozcan, U., Cao, Q., Yilmaz, E., Lee, A.H., Iwakoshi, N.N., Ozdelen, E., Tuncman, G., Görgün, C., Glimcher, L.H., and Hotamisligil, G.S. (2004). Endoplasmic reticulum stress links obesity, insulin action, and type 2 diabetes. Science *306*, 457–461.

Pattacini, L., Mancini, M., Mazzacurati, L., Brusa, G., Benvenuti, M., Martinelli, G., Baccarani, M., and Santucci, M.A. (2004). Endoplasmic reticulum stress initiates apoptotic death induced by STI571 inhibition of p210 bcr-abl tyrosine kinase. Leuk. Res. *28*, 191–202.

Qi, X., and Mochly-Rosen, D. (2008). The PKCdelta -Abl complex communicates ER stress to the mitochondria - an essential step in subsequent apoptosis. J. Cell Sci. *121*, 804–813.

Rosen, E.D. (2005). The transcriptional basis of adipocyte development. Prostaglandins Leukot. Essent. Fatty Acids *73*, 31–34.

Smith, E.R., Lee, M.G., Winter, B., Droz, N.M., Eissenberg, J.C., Shiekhattar, R., and Shilatifard, A. (2008). Drosophila UTX is a histone H3 Lys27 demethylase that colocalizes with the elongating form of RNA polymerase II. Mol. Cell. Biol. *28*, 1041–1046.

Surapureddi, S., Rana, R., Reddy, J.K., and Goldstein, J.A. (2008). Nuclear receptor coactivator 6 mediates the synergistic activation of human cytochrome P-450 2C9 by the constitutive androstane receptor and hepatic nuclear factor-4alpha. Mol. Pharmacol. *74*, 913–923.

Tontonoz, P., Hu, E., and Spiegelman, B.M. (1994). Stimulation of adipogenesis in fibroblasts by PPAR gamma 2, a lipid-activated transcription factor. Cell *79*, 1147–1156.

Tontonoz, P., Nagy, L., Alvarez, J.G., Thomazy, V.A., and Evans, R.M. (1998). PPARgamma promotes monocyte/macrophage differentiation and uptake of oxidized LDL. Cell *93*, 241–252.

Vidal-Puig, A., Jimenez-Liñan, M., Lowell, B.B., Hamann, A., Hu, E., Spiegelman, B., Flier, J.S., and Moller, D.E. (1996). Regulation of PPAR gamma gene expression by nutrition and obesity in rodents. J. Clin. Invest. *97*, 2553–2561.